Received: 12 March 2023 | Revised: 11 April 2023 | Accepted: 27 May 2023

DOI: 10.5185/amlett.2023.041735

OPEN ACCESS

RESEARCH

Effect of *Mangifera indica* extracted CuO NPs on Seed Germination of *Cicer Arietinum* and *Vigna Radiata*: An insight on Biochemical, Physiological and Computational Studies

Ananya Kashyap[1] | Madhubala Kumari[1] | Sumant Kumar[1] | Samira Nazma[1] | Koel Mukherjee[1]* | Dipak Maity[2]*

[1]Department of Bioengineering and Biotechnology, Birla Institute of Technology, Mesra, Ranchi, Jharkhand 835215, India

[2]School of Engineering and Technology, The Assam Kaziranga University, Koraikhowa, NH-37, Jorhat 785006, Assam, India

***Corresponding author:**
Email ID:
dipakmaity@gmail.com
(Dipak Maity)

koelmukherjee@bitmesra.ac.in
(Koel Mukherjee)

ABSTRACT

Biosynthesized metal oxide nanoparticles are used as nano-fertilizers for sustainable agriculture as they have proven to be promising agents in increasing the germination rates and plant growth rate. Biosynthesis of copper oxide nanoparticles (CuO-NPs) was done for the first-time using extract of *Mangifera indica* leaves. Effects of as-synthesized CuO NPs on the seed germination of two legume seeds are investigated at different concentrations (0 - 2.5 mg/ml). UV-Vis and EDX analysis confirm the formation of CuO NPs & FESEM images revealed spherical shape of NPs with particle size ranging from 105nm to 155nm. CuO-NPs also revealed to be highly stable in aqueous suspension with zeta potential value -21.1mV. Germination rate, root /shoot growth and protein estimated of *Cicer arietinum* and *Vigna radiata* seeds found to be highest at 2.5mg/ml and 1mg/ml concentration, respectively. Negative impact on germination rate and root/shoot growth was observed due to toxic effects when CuO-NPs were applied at higher concentration 2.5mg/ml to *Vigna radiata* seeds. Thus, it is concluded that optimum concentration of biosynthesized CuO-NPs can be used to enhance the growth of leguminous seeds because of their possible interaction with the proteins and their up-regulation as confirmed by bioinformatics studies and molecular docking of protein.

KEYWORDS

Copper oxide nanoparticles; biosynthesis; seed germination; *mangifera indica*; legume seeds (Chickpea and Mung)

INTRODUCTION

Nanomaterials (typically 1-100 nm) are well recognized due to their diverse promising application in the field of electronics, food packaging, biomedical and agricultural and other technological sectors [**1-6**]. Nanoparticles (NPs) are greatly successful because of their large surface area and size/shape dependent various unique properties (such as magnetic, electrical, optical, etc.) as compared to their bulk counterparts [**7-10**]. Nowadays green/bio-synthesis of NPs using plant parts like leaves, flowers, fruits, seeds, and roots [**11-16**], and microorganisms [**11,13,17-19**] are preferred over physical/chemical synthesis methods as they are cheaper and less hazardous. An increasing number of studies on biosynthesized NPs and their effects on plants showed improved plant growth and productivity [**12,20**]. Several NPs have been explored to stimulate plants' growth by supplying balanced nutrients like iron, copper, zinc etc. for improving crop quality and yield. Besides, NPs based biofertilizer can also be employed to affect soil fertility and thereby to enhance plants' growth in sustainable agriculture.

Recently, the use of biosynthesized metal oxide nanoparticles (MONPs) as nano-fertilizers, nano-pesticides and nano-biosensors has received a great deal of attention in sustainable agriculture [**21-23**]. MONPs have been demonstrated to be highly promising in boosting seed germination rates, chlorophyll content, stomata regulation, so on. 'Seed germination' can be considered as the destruction of viable seeds dormancy in the accessibility of

This is an open access article licensed under the Creative Commons Attribution 4.0 International License, which allows for use, distribution, and reproduction in any medium as long as the original work is properly cited. The Authors © 2022. The International Association of Advanced Materials, Sweden, publishes Advanced Materials Letters.

favourable conditions. When seeds are developed by the mother plant under a stressful environment for growth, they are modified to a dormant stage, until favourable conditions occur for their development [**24**]. Plants accumulate and store proteins in protein storage vacuoles (PSVs) during seed development and maturation. Upon seed germination, these storage proteins are mobilized to provide nutrients for seedling growth. Similarly, an up-regulation of protein and enzymes such as alpha-amylase protein, pyruvate orthophosphate dikinase, fructokinase phosphoglycerate, pyruvate decarboxylase, allergen RAG2 precursor, putative UDP glucose dehydrogenase, etc. lead to the breaking of seed dormancy [**25**]. Besides, the phytohormones such as gibberellic acids (GA) and abscisic acid (ABA) play an important role in seed dormancy and germination [**27-28**].

Apart from these internal factors, various trace elements and micro-/macro-nutrients are essentially required in the proper seed germination process. Among others, copper (Cu) is extremely important for plants as it acts as a micronutrient and its deficiency may cause different diseases to leave and their flowering organs.

Similarly, a very high amount of copper might damage DNA and causes chlorosis and necrosis of cells, and inhibition of root growth, as it is a high redox transition metal ion [**29**]. Moreover, excess copper in soil competes with other important nutrient uptakes such as iron, zinc, and phosphorus and reduces seed germination and root growth. It also accumulates reactive oxygen species (ROS) and enhances antioxidant activity [**30**]. In addition, copper is also a good antimicrobial agent and could be used to fight against pathogenic microbes due to their both antibacterial and antifungal activity [**31**]. Furthermore, studies are reported that copper NPs can effortlessly adhere to the cell wall and degrade it leading to disruption of the continuous cell wall [**18,32-33**]. Hence the presence of the optimum amount/concentration of copper should be determined in soil for better growth of plants.

The Fabaceae or Leguminosae (commonly known as the legume, pea, or bean) family is the third largest family of flowering plants, consisting of over 20,000 species. A legume refers to any plant from the Fabaceae family that includes its leaves, stems, and pods. Legumes contain various essential components of a balanced vegetarian diet which can prevent certain chronic diseases. Legume seeds are considered a good vegan substitute for animal protein and therefore it is consumed largely in India and in Asian countries.

The effect of green synthesised copper oxide (CuO-NPs) nanoparticles has not been much reported on legume seeds which have nutrient importance to the Indian vegan population. Some reports have been made on the effect of chemically synthesised CuO particles on mung beans [**34-35**]. In this study, firstly efforts are given to the green synthesis of CuO NPs using the extract of mango leaves which are widely available. Secondly, the study focuses on the selection of Hereby, biosynthesized CuO NPs applied to *Vigna radiata* (mung beans) and *Cicer arietinum* (chickpea) seeds at different concentrations (0 – 2.5 mg/ml) to evaluate their effects on seed germination and plant's root/shoot growth. Further, the enzymes involved in seed germination are listed and *in silico* analysis is performed.

EXPERIMENTAL

Materials

All the required chemicals/reagents are of analytical grade and used without any further purification. Anhydrous copper (II) chloride ($CuCl_2$, molecular weight 134.45 grams) was purchased from HiMedia Lab. Young green mango leaves were collected from the campus of Birla Institute of Technology; Mesra. Other reagents like sodium hydroxide, sodium carbonate, copper sulphate, bovine serum albumin, and sodium potassium tartrate and folin ciocalteu were bought from different sources.

Preparation and characterization of mango leaf extract

The fresh mango leaves were washed several times with distilled water to remove dust particles and then air-dried for 2 hours. 20 grams of the cleaned and dried mango leaves were finely cut, weighed, and put into the reagent bottle. After this, 200 ml of distilled water was added to it and the bottle was kept in a water bath for 2-3 hours at a temperature of 60℃. The bottle was removed from the water bath after the leaves becomes decolorized. Next, the bottle was opened and left to cool down to room temperature and the resulting aqueous solution was filtered into a conical flask using Whatman 1 Filter paper. Finally, the obtained mango leaf extract is stored at freezing temperature (-4℃) in the fridge for 2-3 days for further use. A small portion of the extract (~10ml) was used for FTIR analysis.

Biosynthesis of CuO NPs

2.017g of copper (II) chloride ($CuCl_2$) is taken in a 500ml beaker and 150ml of water is added to the beaker. The mixture is heated to 75℃ under constant magnetic stirring to form a homogeneous blue color aqueous $CuCl_2$ solution. The aqueous solution is then heated at the same temperature with constant stirring for about half an hour. Next, the freshly prepared 75 ml of mango leaf extract is warmed up to 45℃ and then added drop-wise to the heated $CuCl_2$ solution under constant magnetic stirring while maintaining the temperature at about 75℃. The color of the solution changes from bluish to brownish black, indicating the gradual formation of CuO-NPs. The resulting mixture solution is then heated at the same temperature for one hour under constant stirring. Later, the supernatant solution is allowed to cool to room temperature and left overnight to allow the CuO NPs for settling down. Then, the mixture solution is centrifuged at 11000 rpm for 10 min and precipitated pellets of CuO NPs are washed with distilled water. Moreover, a small part of the supernatant solution after the centrifugation is decanted and stored in a beaker

for FTIR analysis. This centrifugation and washing procedure are repeated 2-3 times. Finally, half of the washed NPs are dispersed in water and the remaining half is oven dried at 40°C overnight and crushed into powder for further characterization.

Characterization of CuO NPs

As-prepared CuO NPs were characterized using several techniques to determine the structure, morphology (size and shape), surface coatings, particle size distribution and zeta potential. UV-VIS absorption spectrum of the water-dispersed CuO NPs was recorded in the range of 200 - 800 nm using UV-visible spectroscopy (UV/VIS Spectrophotometer 3100-XE- Labindia analytical) while hydrodynamic particle size and zeta potential values of the aqueous suspension of the CuO NPs were measured by dynamic light scattering (DLS- Zetasizer nanoseries Nano ZS, UK). FT-IR spectrum was recorded using ATR (Attenuated total reflection) mode in a wave number range of 4000 – 400 cm^{-1} using a Fourier transform infrared spectroscopy (FTIR, IR Prestige 21, Japan). Finally, FESEM images and EDX analysis of CuO NPs powders were carried out by a field emission scanning electron microscope (FE-SEM, Jeol Japan). XRD of powdered sample was carried out by X-Ray Diffractometer (Rigaku Smart lab X- Ray Diffractometer).

Biochemical/Physiological study of CuO NPs on legume seed germination

The biochemical/physiological effect of the aqueous suspension of CuO nanoparticles were studied on the seed germination of two legume seeds i.e., Mung (*Vigna radiata*) and Chickpea (*Cicer arietinum*). Typically, 30 seeds of mung and 30 seeds of chickpeas were taken in each of 4 Petri plates. Next, 20 ml of the aqueous suspension of CuO nanoparticles at different concentrations (0, 0.5, 1 and 2.5 mg/ml) were added and the experiments were performed in duplicates. After adding the various concentrated NPs solution, the seeds were left for germination for 7-10 days and then different techniques were applied for measurements as mentioned below.

Uptake of CuO NPs by ICP-OES technique

0.5 gram of the seed sample was weighed and put in a 150ml beaker. Then, 10ml of HNO_3 and 1ml of H_2O_2 were added to it. The beaker was kept in boiling water for acid digestion for about 2 hours until the sample was completely dissolved. It was then removed from the water and left for cooling at room temperature. The volume was made up to 100ml by adding distilled water. Finally, 10-15ml of supernatant was taken for ICP-OES analysis [**36**].

Germination rate calculation

Among all seeds, the number of seeds germinated is counted and divided by the total number of seeds.

The germination rate can be calculated by the following formulae which is

$$\text{Germination \%} = \frac{\text{Number of seeds germinated}}{\text{total number of seeds sown for germination}} \times 100$$

Root and shoot length calculation

The root lengths as well as the shoot length of each germinated seed were measured individually by using a millimetre ruler.

Protein estimation

The estimation of protein concentration was determined by the Lowry method based on the complex formation due to the reactivity of divalent copper (II) ions with the peptide bond under an alkaline condition. For example, negative amino acids such as tyrosine, cysteine, and tryptophan react with positive copper ions. Initially, 0.1gm of sodium hydroxide (NaOH) was dissolved in 100ml of distilled water and 2gm of sodium carbonate (Na_2CO_3) was added into this to prepare Reagent A. Then, 1 gram of sodium potassium tartrate was dissolved in 100ml of distilled water and 0.1gram of copper sulphate ($CuSO_4$) was added into this to prepare Reagent B. Next, Reagent C was freshly prepared just before the experiment by combining 1ml of Reagent B with 50ml of Reagent A. Moreover, a standard was prepared by using the BSA.

2 grams of the sample was added to 9ml of distilled water and then finely grounded with a mortar pestle in an ice box to avoid protein degradation. Next, it was centrifuged at 4°C at 10000rpm for 10mins. 1 ml of each sample was added in Test tubes and each test was performed in duplicates. Also, 1 ml of distilled water was taken in a test tube which was served as blank. 4ml of Reagent C is added to each test tube and then left for 10 minutes incubation at room temperature. After 10 mins of incubation, 0.5ml of Folin Ciocalteu was added to each test tube and kept for incubation in the dark at room temperature for 30 min. After incubation OD was taken in Esico (1312) Microprocessor Photo colorimeter at 450 nm against the blank. Protein estimation is done by using the Standard graph prepared earlier.

In silico study

Enzymes involved in the seed germination of legumes were determined based on reported research articles [**37-38**] and pathway databases were cross-checked. Finally, important enzymes related to the seed germination process were shortlisted and Pathways concerned with the seed germination process of leguminous plants were identified and studied using the KEGG pathway database (https://www.genome.jp/kegg/pathway.html). The interactions of these enzymes with different other proteins or enzymes were studied and compared using a STRING database (https://string-db.org/). It was found that beta-amylase in *Cicer arietinum* and *Vigna radiata* is an essential enzyme involved in the seed germination process. Protein sequences of the enzyme beta-amylase were obtained from the NCBI database

(https://www.ncbi.nlm.nih.gov/) in FASTA file format and then a domain search was done using the Pfam site (https://pfam.xfam.org/). At the end, Motif analysis was done using MEME (Multiple Em for Motif Elicitation) Suite software v 5.4.1 (https://meme-suite.org/meme/tools/meme).

RESULTS & DISCUSSION

Fig. 1A shows the UV-Vis absorption spectra of as-prepared biosynthesized NPs and the absorption peak observed at 272 nm confirming formation of CuO NPs [**39**]. **Fig. 1B** depicts the FTIR spectra of mango leaf extract, extract after synthesis (i.e., decanted supernatant solution after the centrifugation) and biosynthesized CuO NPs. The FTIR spectrum at 3315cm^{-1} and at 1600cm^{-1} correspond to the bonds of phenols and alcohols confirms that surface of the CuO NPs is attached with phytochemicals of the mango leaf extract.

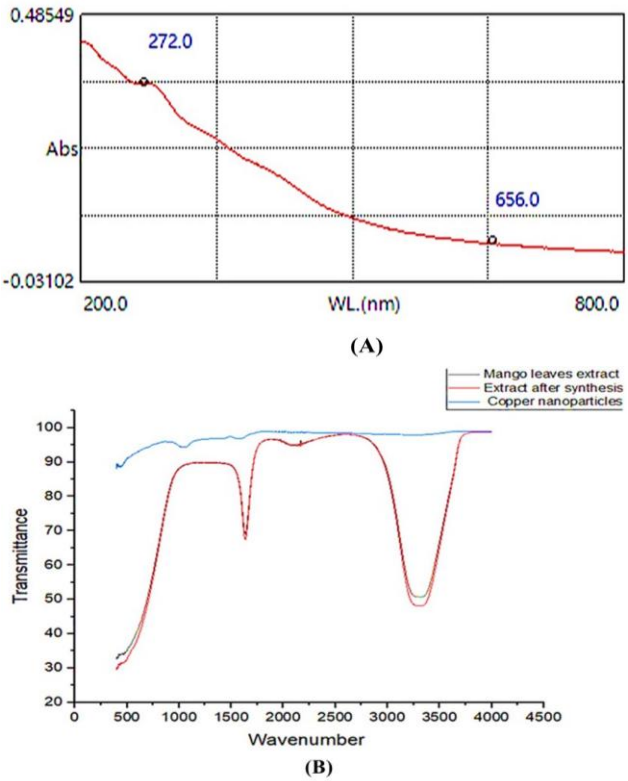

Fig. 1. (A) UV-Visible absorption spectra of biologically synthesized CuO-NPs **(B)** FTIR spectra of mango leaf extract, extract after synthesis/ centrifugation and biosynthesized CuO NPs.

Fig. 2A-C depicts EDX analysis of the as-prepared CuO NPs sample showed the presence of copper and oxygen element beside silicon impurities which could be due to the phytochemicals of the extract used during biosynthesis [**40**]. **Fig. 2D** & **Fig. 2E** shows the FESEM images of biosynthesized CuO NPs. It can be seen that CuO NPs are of nearly spherical shaped with sizes ranging from 105 nm to 155 nm.

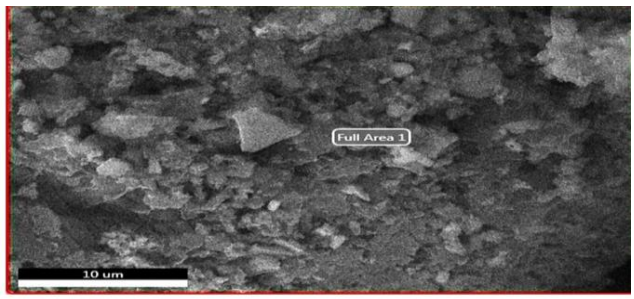

(A)

Element	Weight %	Atomic %	Net Int.	Error %	Kratio	Z	R	A	F
C K	25.84	41.00	51.91	13.39	0.0634	1.1054	0.9387	0.2222	1.0000
O K	37.03	44.12	143.38	10.49	0.1020	1.0601	0.9610	0.2598	1.0000
Al K	0.84	0.59	7.15	41.03	0.0041	0.9462	1.0034	0.5080	1.0057
Si K	4.26	2.89	45.20	10.54	0.0265	0.9674	1.0104	0.6376	1.0070
P K	0.80	0.49	7.87	47.22	0.0054	0.9296	1.0170	0.7158	1.0109
Cl K	4.08	2.19	42.11	8.15	0.0326	0.9024	1.0292	0.8703	1.0187
Fe K	13.66	4.66	54.47	8.48	0.1259	0.8177	1.0669	1.0110	1.1146
Cu K	13.50	4.05	30.80	11.90	0.1129	0.7835	1.0700	0.9982	1.0694

(B)

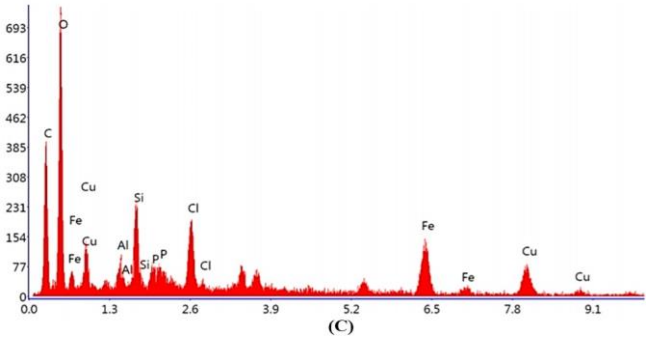

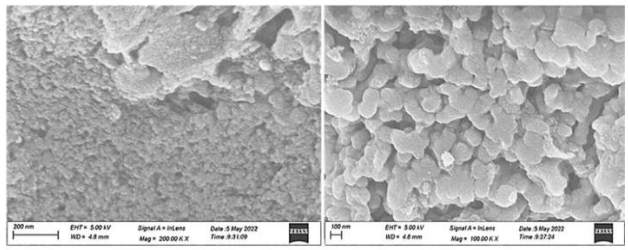

(D)

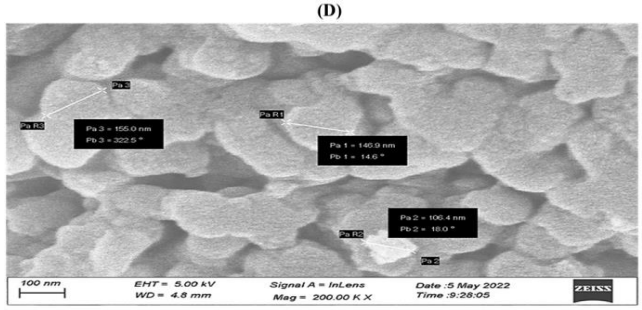

(E)

Fig 2. Image of the CuO-NPs sample for EDX analysis **(A)** Morphological image of CuO-NPs **(B)** Table showing various elemental quantitative result along with weight and atomic percentage present in the CuO-NPs **(C)** EDX spectra of then biosynthesized CuO-NPs **(D&E)** FESEM images of biosynthesized CuO NPs at different magnifications.

Fig. 3A shows the DLS plot of biosynthesized CuO NPs dispersed in aqueous suspension. It can be seen that CuO NPs have broad size distribution ranging between 90 nm and 530nm (i.e., polydisperse). About 37% particles have the hydrodynamic size below 200 nm and 33% particles have hydrodynamic size in the range of 220nm to 295nm. **Fig. 3B** depicts the zeta potential value of -21.1mV indicating stable aqueous suspension of biosynthesized CuO NPs. **Fig 3C** shows results of XRD confirming the CuO NPs. One peak is between 38 degree and the other ranges in between 42 and 50 respectively, which might not be equal to but nearly similar to the peaks as discussed by Singh *et. al.*, 2016 [**41**].

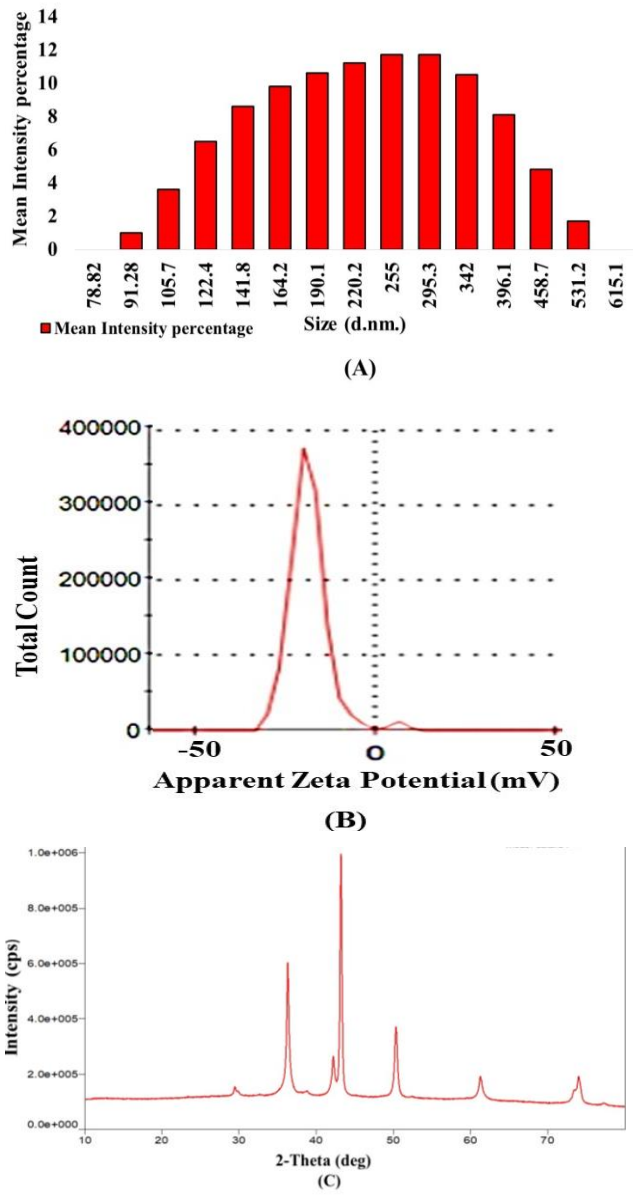

Fig 3. (A) DLS particle size distribution plot **(B)** Zeta potential distribution plot of biosynthesized CuO nanoparticles dispersed in aqueous suspension. **(C)** XRD result of CuO NPs.

Table 1 shows the ICP-OES analysis for the uptake of CuO NPs by *Vigna radiata* and *Cicer arietinum* seeds at different concentrations of (0 - 2.5 mg/ml). It can be seen that uptake of CuO NPs increased with the concentrations up to 2.5mg/ml as compared to the control (i.e., 0 mg/ml) both the seeds. This indicates that CuO NPs are responsible for the changes that happened in seeds applied to them [**37, 42**]. Moreover, uptake of CuO NPs is found to be higher for *Vigna radiata* seeds than *Cicer arietinum* seeds at any concentration other than control.

Table 1. ICP-OES analysis for the uptake of CuO NPs by *Vigna radiata* and *Cicer arietinum* seeds at different concentrations (0 - 2.5 mg/ml).

Sample analyte	Concentration	Mean uptake of Cu in conc. in 15ml of sample
Vigna radiata	Control	0.020 mg/L
	0.5mg/ml	0.278 mg/L
	1mg/ml	0.246 mg/L
	2.5 mg/ml	0.857 mg/L
Cicer arietinum	Control	0.014 mg/L
	0.5mg/ml	0.149 mg/L
	1mg/ml	0.170 mg/L
	2.5 mg/ml	0.223 mg/L

Fig. 4A and **Fig. 4B** show the seed germination images of *Cicer arietinum* (chickpea) and *Vigna radiata* (mung) seeds respectively and **Fig. 4C** depict the plot of corresponding seed germination rate when different concentrations of CuO NPs (0 – 2.5 mg/ml) are applied. It can be seen that the seed germination rate of *Vigna radiata* seeds is gradually increased with the concentration of CuO NPs with respect to the control (i.e., 0 mg/ml) and found to be maximum at 1mg/ml concentration (and then decreased at 2.5 mg/ml concentration). On the other hand, the seed germination rate of the *Cicer arietinum* seeds is initially decreased at 0.5 mg/ml concentration with respect to the control and then gradually increased up to 2.5mg/ml concentration of CuO NPs. Thus, the germination rate of *Vigna radiata* seeds is found to be relatively better at low concentration of CuO NPs (up to 1 mg/ml) than that of the *Cicer arietinum* seeds. On contrary, the germination rate of *Cicer arietinum* seeds is found to be better at higher

concentration of CuO NPs (2.5 mg/ml) than that of the *Vigna radiata* seeds.

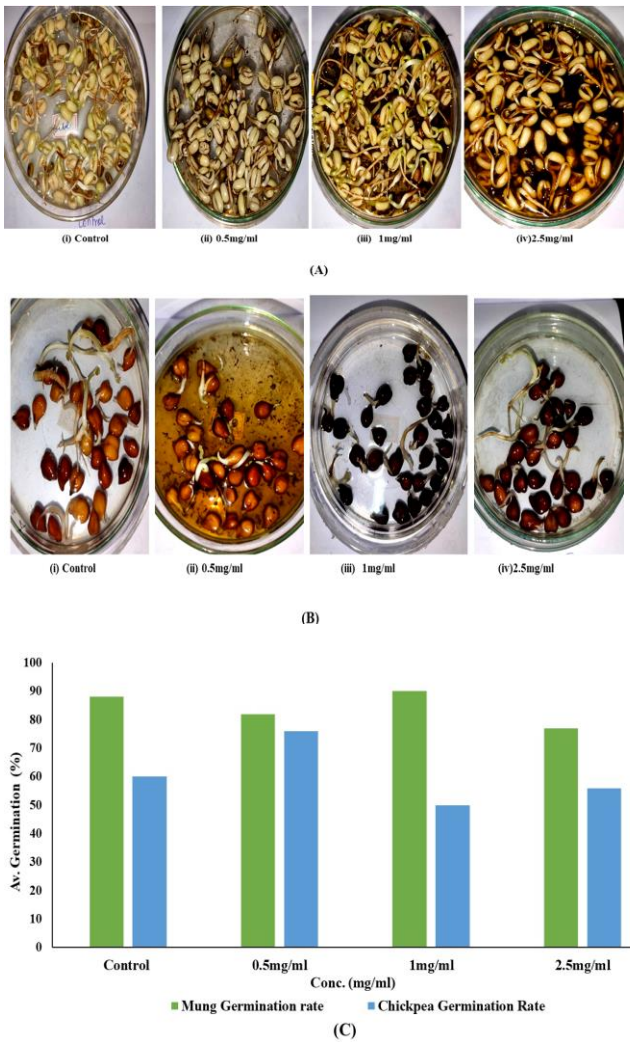

Fig. 4. (A) and **(B)** represent the seed germination images of *Vigna radiata* (mung) and *Cicer arietinum* (chickpea) seeds at different concentrations of CuO NPs (0 – 2.5 mg/ml), respectively. **(C)** shows corresponding seed germination rate plots for *Cicer arietinum* and *Vigna radiata* seeds at different concentrations of CuO NPs.

Fig. 5A shows the images of root and shoots growth of *Vigna radiata* and *Cicer arietinum* seeds at different concentrations of CuO NPs (0.5 mg/ml, 1mg/ml, 2.5 mg/ml). **Fig. 5B** depicts the corresponding root and shoots length of the *Vigna radiata* and *Cicer arietinum* seeds at different concentrations. It can be seen that both the root and shoot length of *Vigna radiata* seeds is gradually increased with the concentration of CuO NPs with respect to the control (i.e., 0 mg/ml) and found to be maximum growth at 1mg/ml concentration (and then decreased at 2.5 mg/ml concentration). On the other hand, both the root and shoot length of the *Cicer arietinum* seeds gradually increased up to 2.5mg/ml concentration of CuO NPs. Moreover, longer root/shoot length (i.e., higher root/shoot growth) is observed for *Vigna radiata* seeds up to 1 mg/ml concentration than that of the *Cicer arietinum* seeds while better root/shoot length is noted for *Cicer arietinum* at 2.5 mg/ml concentration of CuO NPs.

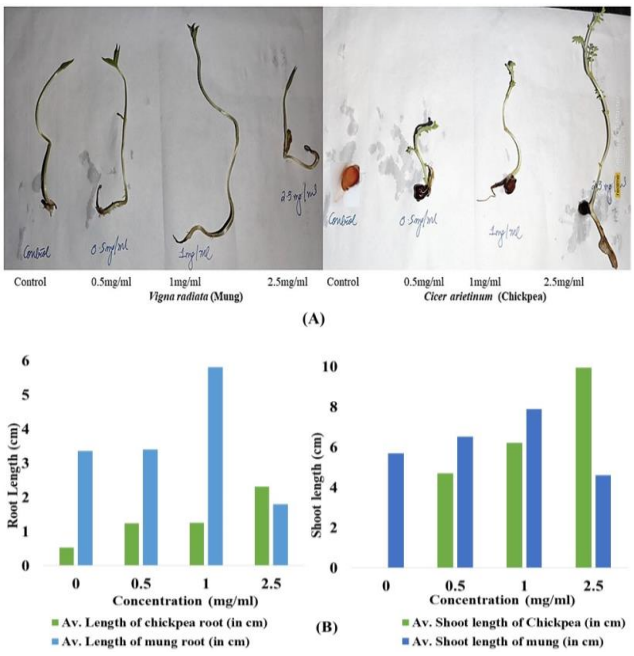

Fig. 5 (A) Represents images of root and shoot growth of *Vigna radiata* and *Cicer arietinum* seeds at different concentrations of CuO NPs (0 - 2.5 mg/ml) **(B)** represents graphical plots based on the measurement of root and shoot length of *Vigna radiata* and *Cicer arietinum* seeds at different concentrations.

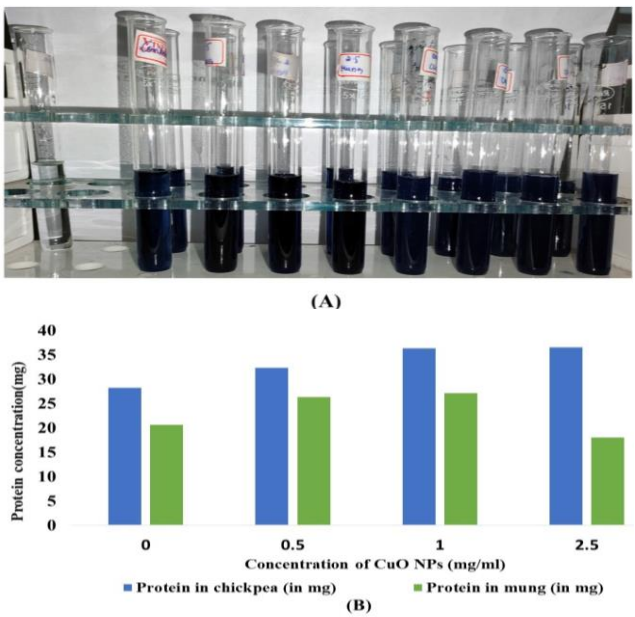

Fig. 6. (A) Images of chickpea and mung seeds samples subjected to Lowry's method after being treated with different concentration of CuO Nanoparticles (0.5 – 2.5mg/ml). **(B)** Graphical representation of the estimated protein amount in *Vigna radiata* and *Cicer arietinum* at various concentrations of CuO NPs.

After performing physiological estimation, biochemical analysis is performed by protein estimation. **Fig. 6A** shows the images of chickpea and mung seeds samples used for protein estimation via Lowry's method. **Fig. 6B** represents the amount of protein in *Vigna radiata* and *Cicer arietinum* seeds samples treated with various concentrations of CuO NPs. It can be seen that amount of protein in *Vigna radiata* seeds gradually increased up to 1mg/ml concentration of CuO NPs and then decreased at 2.5 mg/ml concentration as compared to the control. However, amount of in *Cicer arietinum* seeds protein is gradually increased up to 2.5 mg/ml of CuO NPs as compared to the control. Moreover, higher amount of protein is observed in *Cicer arietinum* seeds than that of the *Vigna radiata* seeds at any concentration (0-2.5 mg/ml). Thus, we can infer that the protein is the key factor to affect the germination rate and root/shoot length which can be improved by applying optimum concentration of CuO NPs to both the *Cicer arietinum* and *Vigna radiata* seeds. Furthermore, higher concentration of CuO NPs can **produce** negative impact on the germination rate and root/shoot growth due to toxic effects to the seeds/plants.

Fig. 7A shows the KEGG pathway of seed germination pathways belonging to legumes family and the results revealed that "Starch and Sucrose metabolism" is an important pathway concerned with seed germination in leguminous plants. The results exhibited that alpha-amylase and beta-amylase play an important role in the seed germination process. **Fig. 7B** depicts the protein-protein interaction of these enzymes with other enzymes using STRING database and the results showed that beta-amylase is a key enzyme responsible for the seed germination pathway in leguminous plants. It was observed that there are strong interactions (score: 0.999-0.998) among the target enzyme beta-amylase (A0A1S3TV97) and other 11 proteins listed in fig. 7 B. All the enzymes are involved in the Starch and Sucrose Metabolism pathway (starch catabolic, metabolic as well as starch biosynthesis processes).

In **Fig. 7 C-D** conserved motif and domain analysis for the beta-amylase enzyme was performed using MEME suit software version 5.4.1. The Conserved domains used in the classification of beta-amylase of *Vigna radiata* (mung beans) and *Cicer arietinum* (chickpea), namely Glycosyl hydrolase family 14 (pfam01373) in beta-amylase sequence were identified by performing an NCBI protein BLAST search. The primary structure analysis of Beta-amylase enzymes included amino acid distribution, motif, and domain analysis. The retrieved FASTA file format amino acid sequence of Beta-amylase enzyme from the NCBI database was subjected to MEME suite software version 5.4.1 and a detailed analysis of motif regions was obtained. A total of 71 motifs were observed in five different sequences of Beta-amylase enzyme responsible for seed germination of *V. radiata* and *C. arietinum* each when subjected to MEME suite software. The motif with width and best possible match amino acid sequences were displayed in the results of MEME suite software. The motif number 1 to 10 (except 8), 12, 13 and 20, (**Fig. 7C** & **Fig. 7D**) were uniformly observed in all the sequences. Motif Number 18 was present in five Beta amylase enzymes (Beta-amylase with 496 residues of amino acid, Beta-amylase 3 chloroplastic, Beta-amylase 1 chloroplastic of *V. radiata* and Beta-amylase with 496 residues of amino acid, Beta-amylase 3 chloroplastic of *C. arietinum*) whereas motif number 16 and 17 were present in 4 sequences of Beta amylase enzyme including Beta-amylase 7 isoform X4 and Beta-amylase 8 of *V. radiata* and Beta-amylase 7 isoform X1 and Beta-amylase 8 of *C. arietinum*. Motif number 11 and 19 were present in 3 sequences of Beta-amylase including Beta-amylase 8 of *V. radiata* and Beta-amylase 7 isoform X1, Beta-amylase 8 of *C. arietinum.* The remaining motifs were present in only two sequences of Beta-amylase enzyme sequences. It can be inferred that the conserved motifs of beta amylase is present in both the legume seeds, and CuO NPs elevated the expressions of the beta –amylase enzyme in both the seeds which in turn responsible for the better seed germination as well as root / shoot development.

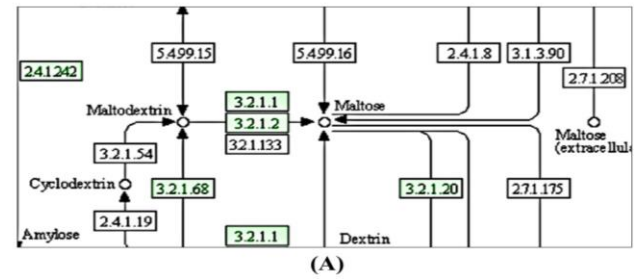

(A)

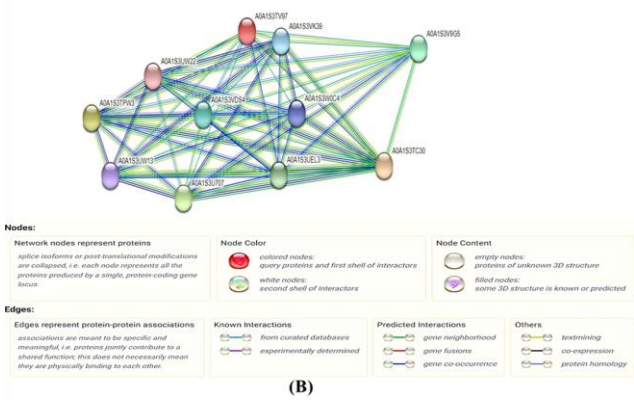

(B)

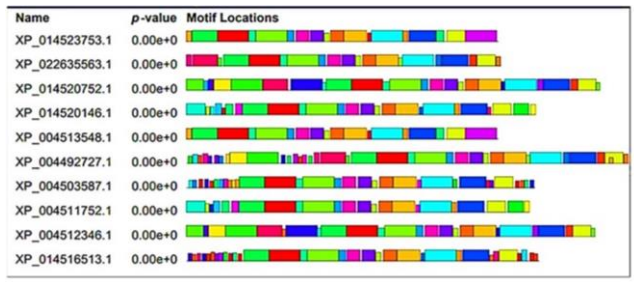

(C)

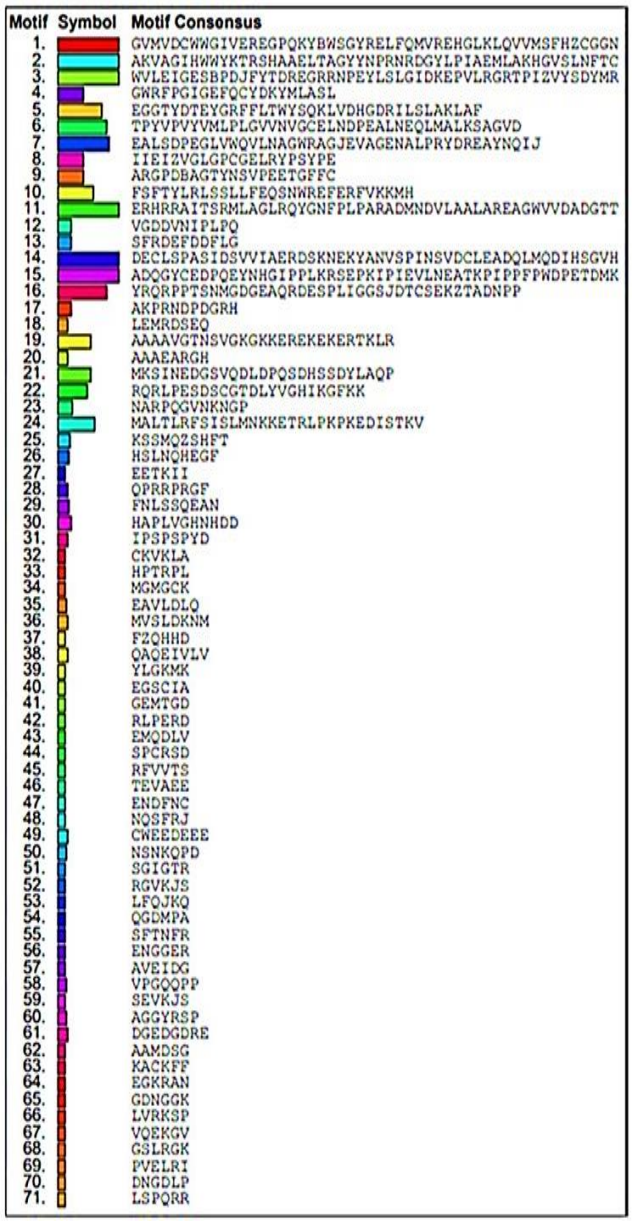

(D)

Fig. 7. (A) Pathway involving Beta-amylase (EC 3.2.1.2) enzyme (red box) for seed germination in legumes **(B)** Protein-protein interaction network of Beta-amylase detected through STRING (PDB ID 1NPC). The red node (A0A1S3TV97) represented Beta-amylase and other nodes represented its predicted functional partners (4-alpha-glucanotransferase DPE2 (A0A1S3TC30), 1,4-alpha-glucan-branching enzyme 1 (A0A1S3TPW3), 1,4-alpha-glucan-branching enzyme 1 (A0A1S3U707), Alpha-amylase (A0A1S3UEL3), Alpha-amylase (A0A1S3V9G5), Beta-amylase (A0A1S3VDS4), Alpha-1,4-glucan phosphorylase (A0A1S3VK39), 1,4-alpha-glucan-branching enzyme 3 (A0A1S3W0C4), Alpha-1,4-glucan phosphorylase (A0A1S3UW13), and Isoamylase 1 (AOA1S3UW22). Occurrence of 71 tandem motifs (with different colour code) among 5 different Beta-amylase enzymes of *Vigna radiata* and *Cicer arietinum* each subjected to MEME **(C)** Motif patterns. First column represents accession no. of enzymes from NCBI database. **(D)** Motif sequences of all individual motifs where first column gives motif numbers, second column for colour code of different motif and third for individual sequence respectively.

CONCLUSION

Biosynthesized CuO NPs is successfully prepared for the first-time using *Mangifera indica* leaf extract and evaluated As-prepared phytochemicals coated CuO NPs are spherical shaped and polydisperse with particle size ranging from 105nm to 155nm as per FESEM analysis and their aqueous suspension is highly stable with zeta potential value -21.1mV. Biosynthesized CuO NPs are applied to legume seeds (Chickpea and Mung) to investigate their effect on seed germination rate and plant growth at different concentrations (0 - 2.5 mg/ml). Germination rate is found to be the highest for *Cicer arietinum* and *Vigna radiata* respectively at 2.5mg/ml and 1mg/ml concentration of CuO NPs. Besides, it was found that the root/shoot length as well as protein estimated amount was found to be gradually increasing until 2.5mg/ml and 1mg/ml concentration for *Cicer arietinum* and *Vigna radiata* seeds respectively. Negative impact on the germination rate, root/shoot and protein concentration growth is observed at higher concentration 2.5mg/ml to the *Vigna radiata* seeds which might be due to toxic effects when CuO NPs that are applied. Thus, it can be concluded that optimal concentration of biosynthesized CuO NPs helps to enhance the growth of leguminous seeds because of their possible interaction with the proteins and up-regulating them as confirmed by the studies based on the bioinformatics of protein and molecular docking of protein. However, further interaction studies on the proteins and enzymes using different bioinformatics tools are needed to understand the effect of CuO NPs on leguminous seeds.

CONFLICT OF INTEREST

Authors don't have any conflict of interest.

ACKNOWLEDGEMENT

The authors are grateful to the Birla Institute of Technology, Mesra for providing infrastructure and financial support (Institute Research Fellowship for Madhubala Kumari) for executing the study. Dipak Maity would like to thank The Assam Kaziranga University for all supports.

REFERENCES

1. Magdassi, S.; Grouchko, M. & Kamyshny, A.; *Materials*, **2010**, *3(9)*, 4626. DOI: 10.3390/ma3094626
2. Souza, V.G.L. & Fernando, A.L. *Food Packaging and Shelf Life* **2016**, *8*, 63. DOI: 10.1016/j.fpsl.2016.04.001
3. Espitia, P.J.P.; Otoni, C.G.; Soares, N.F.F.; In *Antimicrobial food packaging;* Academic Press; **2016**. DOI: 10.1016/B978-0-12-800723-5.00036-X
4. Tortella, G.R.; Pieretti, J.C.; Rubilar, O.; Fernández-Baldo, M.; Benavides-Mendoza, A.; Diez, M.C.; Seabra, A.B. *Critical Reviews in Biotechnology* **2022**, 42(3), 431. DOI: 10.1080/07388551.2021.1939260
5. Gisbert-Garzarán, M.; Vallet-Regí, M.; *Nanomaterials* **2022**, *12(7)*, 1189. DOI: 10.3390/nano12071189
6. Rahman, A.; Chowdhury, M.A.; Hossain, N.; *Applied Surface Science Advances* **2022**, *11*, 100296. DOI: 10.1016/j.apsadv.2022.100296
7. Khan, I.; Saeed, K.; Khan, I.; *Arab J Chem.*, **2019,** *12*, 908. DOI: 10.1016/j.arabjc.2017.05.011

8. Klaine, S.J.; Alvarez, P.J.; Batley, G.E.; Fernandes, T.F.; Handy, R.D.; Lyon, D.Y.; Mahendra, S.; McLaughlin, M.J.; Lead, J.R.; *Environmental Toxicology and Chemistry: An International Journal*, **2008**, *27(9)*, 1825. DOI: https://doi.org/10.1897/08-090.1
9. Maity D.; Ding J.; Xue J-M.; *Functional Materials Letters*, **2008**, *1*, 189. DOI: 10.1142/S1793604708000381
10. Maity D.; Choo S-G.; Yi J.; Ding J.; Xue J-M.; *Journal of Magnetism and Magnetic Materials*, **2009**, *321*, 1256. DOI: 10.1016/j.jmmm.2008.11.013
11. Hasan, S.; *Res. J. Recent Sci.*, **2015**, *2277*, 2502. ISSN 2277-2502
12. Singh, A.; Singh, N.B.; Hussain, I.; Singh, H.; Singh, S.C.; *Int. J. Pharm Sci Invent*, **2015**, *4*(8), 25. ISSN (Online): 2319 – 6718
13. Ovais, M.; Khalil, A.T.; Islam, N.U.; Ahmad, I.; Ayaz, M.; Saravanan, M.; Shinwari, Z.K.; Mukherjee, S.; *Applied Microbiology and Biotechnology*, **2018**, *102*(16), 6799. DOI: https://doi.org/10.1007/s00253-018-9146-7
14. Selvi, V.S.; Velumani, A.; Banu, N.N.; *Journal of Nanoscience and Technology*, **2019**, 784-786. DOI: https://doi.org/10.30799/jnst.240.19050411
15. Rani N.; Rawat K.; Saini M.; Shrivastava A.; Kandasamy G.; Saini K.; Maity D.; *Chemical Papers* **2022**, *76*, 1225. DOI: 10.1007/s11696-021-01942-y
16. Saini M.; Yadav S.; Rani N.; Mushtaq A.; Rawat S.; Saini K.; Maity D.; *Materials Science & Engineering B*, **2022,** 282, 115789. DOI: 10.1016/j.mseb.2022.115789
17. Honary, S.; Barabadi, H.; Gharaei-Fathabad, E.; Naghibi, F.; *Dig J. Nanomater Bios*, **2012**, *7*(3), 999. DOI: ISSN: *1842-3582*
18. Ramyadevi, J.; Jeyasubramanian, K.; Marikani, A.; Rajakumar, G.; Rahuman, A.A.; *Materials Letters*, **2012**, *71*, 114. DOI: 10.1016/j.matlet.2011.12.055
19. Rasool, U.; Hemalatha, S.; *Materials Letters*, **2017**, *194*, 176. DOI: 10.1016/j.matlet.2017.02.055
20. Parveen, A.; Rao, S.; *Journal of Cluster Science*, **2015**, *26*(3), 693. DOI: 10.1007/s10876-014-0728-y
21. Maity, D.; Gupta, U.; Saha, S.; *Nanoscale* **2022**, *14*(38), 13950. DOI: https://doi.org/10.1039/D2NR03944C
22. Arora S.; Murmu G.; Mukherjee K.; Saha S.; Maity, D.; *Journal of Biotechnology*, **2022,** *355*, 21. DOI: 10.1016/j.jbiotec.2022.06.007
23. Singh P.; Tiwari A.; Maity, D.; Saha, S.; *Journal of Materials Science*, **2022,** *57*. 10836. DOI: 10.1007/s10853-022-07259-9
24. Bentsink, L.; Koornneef, M.; *The Arabidopsis Book/American Society of Plant Biologists*, **2008**, *6*. DOI: 10.1199/tab.0119
25. Kaneko, M.; Itoh, H.; Ueguchi-Tanaka, M.; Ashikari, M.; Matsuoka, M.; *Plant Physiology*, **2002**, *128*(4), 1264. DOI: https://doi.org/10.1104/pp.010785
26. Tuan, P.A.; Kumar, R.; Rehal, P.K.; Toora, P.K.; Ayele, B.T.; *Frontiers in Plant Science*, **2018**, *9*, 668. DOI: 10.3389/fpls.2018.00668
27. Han, C.; Yang, P.; *Proteomics*, **2015**, *15*(10), 1671. DOI: 10.1002/pmic.201400375
28. He, D.; Han, C.; Yang, P.; *Journal of Integrative Plant Biology*, **2011**, *53*(10), 835. DOI: 10.1111/j.1744-7909.2011.01074.x
29. Yruela, I.; *Brazilian Journal of Plant Physiology*, **2005**, *17*, 145. DOI: 10.1590/S1677-04202005000100012
30. Mir, A.R.; Pichtel, J.; Hayat, S.; *Biometals*, **2021**, *34*(4), 737. DOI: 10.1007/s10534-021-00306-z
31. Usman, M.S.; El Zowalaty, M.E.; Shameli, K.; Zainuddin, N.; Salama, M.; Ibrahim, N.A.; *International Journal of Nanomedicine*, **2013**, *8*, 4467. DOI: 10.2147/IJN.S50837
32. Raffi, M.; Mehrwan, S.; Bhatti, T.M.; Akhter, J.I.; Hameed, A.; Yawar, W.; *Annals of Microbiology*, **2010**, *60*(1), 75. DOI: https://doi.org/10.1007/s13213-010-0015-6
33. Longano, D.; Ditaranto, N.; Sabbatini, L.; Torsi, L.; Cioffi, N.; In *Nano-antimicrobials*; Springer, Berlin: Heidelberg, **2012**. DOI: 10.1007/978-3-642-24428-5_3
34. Singh, A.; Singh, N.B.; Hussain, I.; Singh, H.; Yadav, V.; *Tropical Plant Research*, **2017**, *4*(2), 246. DOI: 10.22271/tpr.2017.v4.i2.034
35. Rohilla, D.; Chaudhary, S.; Singh, N.; Batish, D.R.; Singh, H.P.; *Environmental Nanotechnology, Monitoring & Management*, **2020**, *14*, 100338. DOI: 10.1016/j.enmm.2020.100338
36. Yan, A.; Chen, Z.; *In (Ed.) New Visions in Plant Science*: Intech Open, **2018**. DOI: https://doi.org/10.5772/INTECHOPEN.74101
37. Ma, Z.; Bykova, N. V.; Igamberdiev, A. U.; *The Crop Journal*, **2017**, *5*(6), 459. DOI: 10.1016/j.cj.2017.08.007
38. Joshi, R.; *International Journal of Creative Research Thoughts*, **2018**, *6*(2), 1481. DOI: ISSN: 2320-2882
39. Ssekatawa, K.; Byarugaba, D. K.; Angwe, M. K.; Wampande, E. M.; Ejobi, F.; Nxumalo, E.; Kirabira, J. B.; *Frontiers in Bioengineering and Biotechnology*, **2022**, *10*, *820218*. DOI: 10.3389/fbioe.2022.820218
40. Rajeshkumar, S.; Malarkodi, C.; *Bioinorganic Chemistry and Applications*, **2014**, *581890*. DOI: 10.1155/2014/581890
41. Singh, J.; Kaur, G.; Rawat, M.; *J. Bioelectron. Nanotechnol*, **2016**, *1*(9). DOI: 10.13188/2475-224X.1000003
42. Raliya, R.; Franke, C.; Chavalmane, S.; Nair, R.; Reed, N.; Biswas, P.; *Frontiers in Plant Science*, **2016**, *7*, 1288. DOI: 10.3389/fpls.2016.01288

This article is licensed under a Creative Commons Attribution 4.0 International License, which allows for use, sharing, adaptation, distribution, and reproduction in any medium or format, as long as appropriate credit is given to the original author(s) and the source, a link to the Creative Commons license is provided, and changes are indicated. Unless otherwise indicated in a credit line to the materials, the images or other third-party materials in this article are included in the article's Creative Commons license. If the materials are not covered by the Creative Commons license and your intended use is not permitted by statutory regulation or exceeds the permitted use, you must seek permission from the copyright holder directly.

Visit http://creativecommons.org/licenses/by/4.0/ to view a copy of this license.